LAWRENCE
LIVERMORE
NATIONAL
LABORATORY

UCRL-JRNL-206515

Generation of Methane in the Earth's Mantle: In situ High P-T Measurements of Carbonate Reduction

H. P. Scott, R. J. Hemley, H.-K. Mao, D. R. Herschbach, L. E. Fried, W. M. Howard, S. Bastea

September 13, 2004

Proceedings of the National Academy of Sciences of the United States of America

Disclaimer

Generation of Methane in the Earth's Mantle: In situ High *P-T* Measurements of Carbonate Reduction

Henry P. Scott[1], Russell J. Hemley[2], Ho-kwang Mao[2], Dudley R. Herschbach[3], Laurence E. Fried[4], W. Michael Howard[4] and Sorin Bastea[5]

[1]Department of Physics and Astronomy, Indiana University South Bend, South Bend, IN 46634

[2]Geophysical Laboratory, 5251 Broad Branch Road NW, Carnegie Institution of Washington, Washington, DC 20015

[3]Department of Chemistry and Chemical Biology, Harvard University, Cambridge, MA 02138

[4]Chemistry and Materials Science Directorate, Lawrence Livermore National Laboratory, Livermore, CA 94550

[5]Physics and Advanced Technologies Directorate, Lawrence Livermore National Laboratory, Livermore, CA 94550

Abstract

We present *in situ* observations of hydrocarbon formation via carbonate reduction at upper mantle pressures and temperatures. Methane was formed from FeO, $CaCO_3$-calcite and water at pressures between 5 and 11 GPa and temperatures ranging from 500 to 1500°C. The results are shown to be consistent with thermodynamic calculations of the relevant chemical reactions based on the thermochemical models and ab initio theory. The study demonstrates the existence of abiogenic pathways for the formation of

hydrocarbons in the Earth's interior and suggests that the hydrocarbon budget of the bulk Earth may be larger than conventionally assumed.

Understanding the speciation of carbon at the high pressures and temperatures that prevail within the Earth has a long and controversial history. It is well known that terrestrial carbon exists in several forms: native, oxidized, and reduced in a wide variety of hydrocarbons. This complexity is demonstrated by many examples: diamonds in kimberlite formations; graphite in metamorphic rocks; CO_2 emission from volcanoes; ubiquitous carbonate minerals in the crust; methane hydrates on the ocean floor; and petroleum reservoirs in sedimentary basins. Of particular interest is the stability and formation of reduced species such as methane and heavier hydrocarbons. The stability, formation, and occurrence of methane under low pressure conditions of the Earth's crust are well-established. Recently, methane and C2-C4 alkanes have been documented to occur in many locations for which isotopic evidence points to an abiogenic origin (*1, 2*), and it has been shown that nickel-iron alloys can catalyze the formation of CH_4 from bicarbonate at conditions relevant to the upper crust (*3*). Yet the evidence is considered to rule out a globally-significant abiogenic source of hydrocarbons (*2*). In contrast, theoretical calculations and experimental data have been presented in support of a persistent assertion that petroleum originates chiefly through abiogenic processes at the high pressures and temperatures found below 100 km (*4*). The experiments, extending to 5 GPa and 1200 °C, involved mass spectroscopic analysis of quenched samples and found methane and smaller amounts of C2-C6 hydrocarbons. We report here the first *in situ* high *P-T* experiments to show that methane readily forms by reduction of carbonate under conditions typical for the Earth's upper mantle. The results may have significant implications for the hydrocarbon budget at depth in the planet.

Many factors are known to control the stability of carbon-bearing phases in the C-O-H system including pressure, temperature, C/H ratio and oxidation state, and it has long been appreciated that the relevant species in this system are C, O_2, H_2, CO, CO_2, CH_4, and H_2O (*5*). At low pressures this system is well understood, and available thermodynamic databases can accurately predict phase stability. For example, studies of

the C-O-H system in relation to crustal fluids and fluid inclusions have been carried out using well-established techniques (*5, 6*). Notably, theoretical modeling is both thermodynamically and observationally consistent at pressures less than about 1 GPa (*7*); however, at higher pressures the system is poorly constrained (*8*), and little experimental work has been done to investigate equilibria between various carbon phases under the high pressure conditions of the upper mantle. In particular, previous experimental and theoretical work has shown that methane may be an important fluid phase at pressures of up to 1 GPa and low oxygen fugacities. It has been shown that methane may be the dominant C-bearing fluid phase at substantially reducing conditions (*6*), and that meteorite hydrocarbons can be formed by the thermal decomposition of $FeCO_3$-siderite (*9*). The importance of pressure is straightforward as it increases by ~1 GPa (10 kbar) for every 30 km of depth in the Earth. Kimberlite eruptions, for example, typically come from depths near 150 km (5 GPa). Higher-pressure work has been completed on the effects of various species in the C-O-H system on the melt characteristics of mantle minerals (*10, 11*), but this does not directly assess the stability of carbon-bearing phases.

We have conducted *in situ* high *P-T* experiments specifically designed to detect methane formation under geologically relevant conditions for the Earth's upper mantle. Starting materials were natural $CaCO_3$–calcite, FeO–wüstite, and distilled H_2O. Experiments were conducted using new diamond anvil cell (DAC) techniques: simultaneous high pressure and high temperature conditions were produced by both resistive (*12*) ($T<600°C$) and laser heating ($T>1{,}000°C$) methods. We utilized three different laser heating systems, including both single- and double-sided and both CO_2 and Nd-YLF lasers (*13, 14*). *In situ* analyses were made by a combination of Raman spectroscopy, synchrotron x-ray diffraction, and optical microscopy. *In situ* Raman spectroscopy proved essential because of its high sensitivity for the C–H stretching vibrations diagnostic of molecular species; it was also useful for examining amorphous or poorly crystalline phases. The synchrotron x-ray diffraction provided a means to identify crystalline phases and help determine the reactions. Both techniques allow precise spatial resolution for probing 5-10 μm diameter regions of the sample chamber; this was of particular importance for these experiments due to the heterogeneous nature of the samples.

Representative Raman spectra exhibiting the presence of bulk methane from two experiments are shown in Fig. 1. Both spectra are dominated by the broad O-H stretching vibration of H_2O, but clearly indicate the presence of a hydrocarbon species with a C-H stretching vibration near 2950 cm^{-1}. For both experiments, a molar ratio of 8:1 (FeO: calcite), excess H_2O, and a mean grain size of ~1 μm was used for starting material. For example, as seen in Fig. 1a, hydrocarbon-rich regions are found after laser heating at ~1500°C at 5.7 GPa. The hydrocarbon is clearly identified as methane based on the sharp band at 2972 cm^{-1} matching the position of bulk methane at this pressure (*15*). The broad feature near 3200 cm^{-1} is due to O-H stretching in ice VII (*16*). This sample exhibited considerable heterogeneity; Raman measurements of laser-heated experiments were typically challenging because after heating the samples were fine-grained, fluorescent, and a layer of opaque material across the diamond surface often obscured the interior of the sample chamber from optical measurements. It is important to note that the diamond anvils do not show evidence of reaction with the sample material.

We have found that the extremely high temperatures of laser heating are not necessary for methane formation. The spectrum in Fig. 1b was collected *in situ* at 600°C. Resistive heating was initiated at 5.1 GPa, and the temperature was ramped at a rate of 50°/minute. The C-H stretching band was apparent by 500°C, becoming very strong by 600°C. This spectral feature was ubiquitous in the sample chamber. The O-H stretching vibration at 3475 cm^{-1} is due to the liquid phase of H_2O. Indeed, it appears that methane formation proceeds much more readily in the lower temperature experiments.

In situ synchrotron x-ray diffraction was used to constrain the principal reaction. The possible reactions include the following:

$$8\ FeO + CaCO_3 + 2\ H_2O = 4\ Fe_2O_3 + CH_4 + CaO \qquad (1)$$

$$9\ FeO + CaCO_3 + 2\ H_2O = 3\ Fe_3O_4 + CH_4 + CaO \qquad (2)$$

Figure 2 shows powder diffraction from a sample after pressure and temperature quench. The one-dimensional pattern is dominated by Fe_3O_4-magnetite, but weak diffraction lines

of another, likely Ca-bearing, phase are present as well. Notably, on the two-dimensional detector image from which this pattern was derived, it is clear that these lines are from spotty diffraction rings; this indicates a coarsely crystalline nature, and phase identification is accordingly difficult. The presence of abundant magnetite strongly favors a reaction such as Eq. (2), but the diffraction data are inconsistent with a chemically-simple phase such as CaO or $Ca(OH)_2$, and suggest a calcium ferrite chemistry such as $CaFe_5O_7$, $CaFe_4O_7$, or $CaFe_2O_4$.

Additional information was obtained from *in situ* optical microscopy carried out in conjunction with the spectroscopy and diffraction. Indeed, detailed examination of the samples as a function of pressure and temperature revealed characteristic changes of methane formation. Most notable was the extensive bubble formation, shown in Fig. 3, indicative that accompanied decompression of the samples. Despite the low density of bubbles, micro-Raman measurements indicate that they are predominantly methane. Figure 3 shows a spectrum from a bubble collected after decompressing a sample that was heated at 5.7 GPa; a very weak feature attributable to methane is observed. Also significant is the fact that none of our experiments at pressures greater than 10 GPa have been successful in producing quality Raman spectra. However, all experiments have displayed bubble growth on decompression to pressures below 1 GPa. Therefore, the formation of methane may be widespread in the experiments to date, but dispersed throughout the sample chamber in low enough concentration that detection is difficult until the H_2O –ice melts and the two phases separate.

Further insight into the chemical processes involved in high pressure methane production may be obtained through new thermochemical modeling. Our aim is to address the temperature and pressure dependence of the methane forming reaction; specifically, it is important to determine if the high-pressure formation of methane is indeed favored at lower temperatures, or if this is an experimental artifact (laser versus resistive heating). High-pressure chemical equilibrium was calculated with the Cheetah (*17*) thermochemical code. The calculations employed a single fluid phase of variable chemical composition in equilibrium with several solid phases. Species in the fluid phase were treated with a spherical exponential-6 fluid model. Species in the solid phase were treated with simple or extended Murnaghan equations of state (*18*); the Scaled Particle

Theory (SPT) / Simplified Perturbed Hard Chain Theory (SPHCT) calculations of Kenney et al (*4*) do not consider solid phases and have a more limited pressure range than the Cheetah code.

The following species were considered for the fluid phase: C,H, H_2, O, O_2, O_3,Fe,Ca,CaO, CH_4,C_2H_6,C_2H_4,C_2H_2,H_2O,CO,CO_2,CH_3OH, and C_2H_5OH.

The following solid species were considered for the condensed phases: Ca(I), Ca(II), CaO(B1), CaO(B2), $CaCO_3$(calcite), $CaCO_3$(aragonite), C(diamond), C(graphite), Fe, FeO(B1), Fe_2O_3, Fe_2O_3(II), Fe_3O_4(magnetite), and Fe_3O_4(h-phase). Several liquid phase species were also considered in the calculations: Ca, Fe, C, FeO, $CaCO_3$ and CaO. Our calculations assumed full chemical equilibrium (i.e., representing a hypothetical experiment conducted for an infinite amount of time). Chemical equilibrium calculations are appropriate to the high temperature experiments reported here, where most reactions are assumed to be fast compared to the timescale of the experiment.

Figure 4 shows the concentration of species for an 8:1:20 molar ratio of FeO, $CaCO_3$, and H_2O at 500° C. Hydrocarbons are found for pressures lower than 8 GPa. This suggests that the experimental weakness of the Raman signature of methane at high pressure is due to a shifting chemical equilibrium, in addition to the phase separation observed. The only hydrocarbon species with significant concentration is CH_4. Its concentration is substantial for pressures up to 2 GPa. Molecular hydrogen is predicted to accompany CH_4. Hydrogen dominates at low pressures, while the hydrogen and CH_4 concentrations become comparable at pressures over 1 GPa. Hydrogen is formed in our calculations from the breakdown of FeO:

$$3FeO + H_2O = Fe_3O_4 + H_2 \qquad (3)$$

The varying H_2 concentrations are due mostly to the equilibrium of reaction (3). In calculations of a 4:10 molar mixture of FeO/water at 500º C, we find that decomposition is nearly complete at low pressures, while at pressures over 5 GPa almost no decomposition (and concomitant production of hydrogen) is found. Although we have not detected H_2 experimentally, it may be dispersed at a concentration below our detection limit, or it may react with and enter the gasket material.

The calculations predicted that the concentrations of CaO and CH_4 were nearly equal at 500º C, suggesting the following decomposition mechanism for $CaCO_3$:

$$4H_2 + CaCO_3 = CH_4 + CaO + 2H_2O. \quad (4)$$

Carbon in the form of graphite or diamond is not predicted to form at 500º C at any pressure considered. Calcite is predicted to convert to aragonite at pressures over 1 GPa. Aragonite and FeO are predicted to be stable to decomposition at pressures over 7 GPa.

Our calculations show that methane production is disfavored at higher temperatures. Figure 4b shows the concentration of species for the mixture at 1500º C. In this case the CaO concentration is found to be nearly equal to the CO_2 concentration. This is in contrast to the calculation at 500º C, where the CO_2 concentration was negligible. The results indicate the following decomposition mechanism

$$CaCO_3 = CaO + CO_2. \quad (5)$$

If we subtract the high-temperature mechanism (5) from the low-temperature mechanism (4), we are left with the well-known methane reforming reaction:

$$4H_2 + CO_2 = CH_4 + 2H_2O. \quad (6)$$

Significant quantities of CO associated with partial oxidation in the reforming reaction are also found at higher temperatures as shown in Fig. 4b. High temperatures favor H_2 and CO_2, while lower temperatures favor CH_4 and H_2O. In calculations of a 10% molar ratio of H_2O to CO_2, we find that methane formation is favored under 1200º C at 1 GPa, while H_2 formation is favored over 1200º C. In Figure 4b the concentrations of magnetite and H_2 are nearly equal at 1500º C, indicating the dominance of reaction (3).

Chemical equilibrium calculations on a representative 1:10 molar mixture of CH_4 and H_2O were also performed with the CHEQ thermochemical code (*19*) to determine if fluid-fluid phase separation is thermodynamically favored at the experimental conditions. The CHEQ code does not include the solid phases considered in the Cheetah modeling, but has the ability to determine chemical equilibrium between several mixed fluid phases. The major fluid species allowed were the same as in the Cheetah code. The results indicate that a separation into CH_4-rich and H_2O-rich phases should be favored at all pressures for temperatures less than ~700º C, while at 1500º C pressures of more than ~23 GPa are predicted to be necessary to induce phase separation. These results are in agreement with the formation of methane bubbles that we observe upon decompression and cooling to room temperature of the diamond anvil cell.

The results of our *in situ* experiments and thermochemical modeling differ markedly from those obtained by quenching (*4*), which found the yield of methane at 4 GPa from FeO + $CaCO_3$ + H_2O was very small at 600 °C and below but climbed steadily up to 1200 °C. The previous thermochemical calculations (*4*) do not pertain to this experimental reactant mixture but rather treat the formation of higher hydrocarbons from an assumed supply of methane.

In conclusion, we present the first *in situ* observations of methane formation at the high pressures and temperatures of the Earth's upper mantle. Methane is expected to form inorganically from any carbonate species, such as $FeCO_3$-siderite or $MgCO_3$-magnesite, in the presence of H_2O at oxygen fugacities near the wüstite-magnetite fO_2 buffer. Such conditions may be widespread in the mantle, and can be moderated by the presence of iron-bearing phases such as Fe_2SiO_4-fayalite, FeS-troilite, or accessory minerals such as $FeCr_2O_4$-chromite and $FeTiO_3$-ilmenite. Thermochemical calculations show that methane production is thermodynamically favorable under a broad range of high pressure-temperature conditions. The calculations indicate that methane production is most favored at 500ºC and pressures less than 7 GPa; higher temperatures are expected to lead to CO_2 and CO production through a reforming equilibrium with methane. The experimental results indicate the methane stability field is significantly expanded at high pressures. These results have broad implications for the hydrocarbon budget of the planet, and indicate that methane may be a more prevalent carbon-bearing phase in the mantle than previously thought, with implications for the deep hot biosphere (*20*). The potential may exist for the high-pressure formation of heavier hydrocarbons using mantle-generated methane as a precursor.

Experimental

Diamond anvil cells with anvil culets ranging between 350–700 μm in diameter were used. Sample chambers were constructed by drilling a hole approximately 70% of the culet diameter into an initially 260 μm thick spring steel foil which was used as a gasket material; the gaskets were pre-indented prior to drilling to a thickness of about 60 μm. Pressure was measured by use of the ruby fluorescence technique (*21*). CO_2 and double-side Nd-YLF laser heating experiments and Raman scattering and optical microscopy analyses were performed at the Geophysical Laboratory (*13, 14*). Pyrometry was used to

determine sample temperature in selected runs. The x-ray measurements and double-sided Nd-YLF laser heating were performed using the HPCAT facilities of APS (Advanced Photon Source, Argonne National Laboratory).

Acknowledgement
Portions of this research work were performed under the auspices of the U.S. Department of Energy by the University of California, LLNL under contract number W-7405-Eng-48.

References

1. B. Sherwood Lollar *et al.*, *Geochim. Cosmochim. Acta* **57**, 5087 (1993).
2. B. Sherwood Lollar, T. D. Westgate, J. A. Ward, G. F. Slater, G. Lacrampe-Couloume, *Nature* **416**, 522 (2002).
3. J. Horita, M. E. Berndt, *Science* **285**, 1055 (1999).
4. J. F. Kenney, V. A. Kutcherov, N. A. Bendeliani, V. A. Alekseev, *Proc. Nat. Acad. Sci.* **99**, 10976 (2002).
5. J. R. Holloway, *Geology* **12**, 455 (1984).
6. B. M. French, *Rev. Geophys.* **4**, 223 (1966).
7. J. M. Huizenga, *Lithos* **55**, 101 (2001).
8. D. J. Frost, B. J. Wood, *Contrib. Mineral. Petrol.* **121**, 303 (1995).
9. T. M. McCollom, *Geochim. Cosmochim. Acta* **67**, 311 (2003).
10. D. H. Eggler, D. R. Baker, in *High-Pressure Research in Geophysics (Advances in Earth and Planetary Sciences, v. 12)* S. Akimoto, H. M. Manghnani, Eds. (Tokyo, 1982) pp. 237-250.
11. S. Jakobsson, J. R. Holloway, *J. Volcanol. Geotherm. Res.* **29**, 265 (1986).
12. W. A. Bassett, A. H. Shen, M. Bucknum, I. M. Chou, *Rev. Sci. Instrum.* **64**, 2340 (1993).
13. Y. Ma *et al.*, *Rev. Sci. Instrum.* **72**, 1302 (2001).
14. O. Tschauner, H. K. Mao, R. J. Hemley, *Phys. Rev. Lett.* **87**, 075701 (2001).
15. P. Hebert, A. Polian, P. Loubeyre, R. Le Toullec, *Phys. Rev. B* **36**, 9196 (1987).
16. G. A. Walrafen, M. Abebe, F. A. Mauer, S. Block, G. J. Piermarini, *J. Chem. Phys.* **77**, 2166 (1982).
17. L. E. Fried, W. M. Howard, *J. Chem. Phys.* **110**, 12023 (1999).
18. L. E. Fried, W. M. Howard, *Phys. Rev. B* **61**, 8734 (2000).
19. F. H. Ree, *J. Chem. Phys.* **81**, 1251 (1984).
20. T. Gold, *The Deep Hot Biosphere* (Copernicus, New York, 1999), pp. 235.
21. H. K. Mao, P. M. Bell, J. W. Shaner, D. J. Steinberg, *J. Appl. Phys.* **49**, 3276 (1978).

Figures and Captions

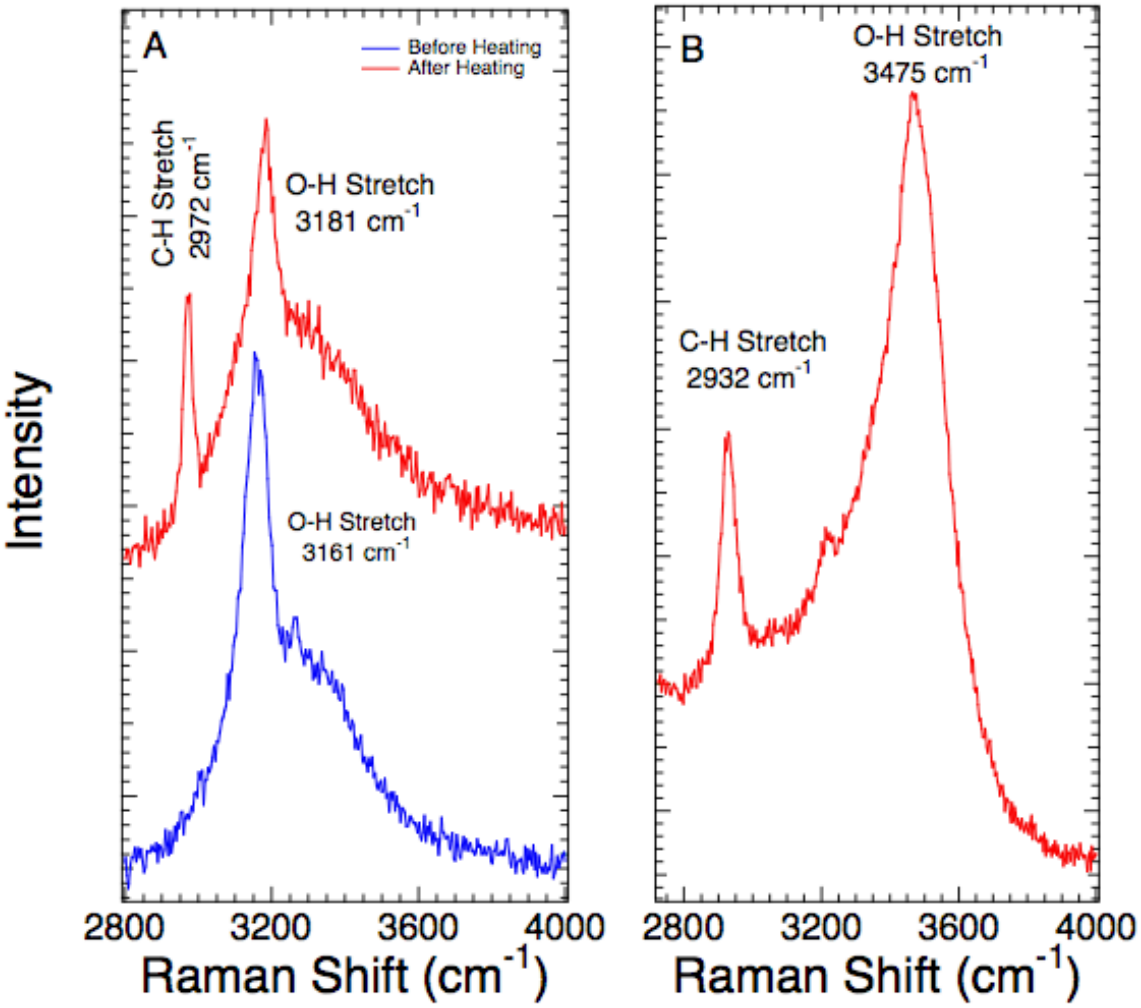

Figure 1: Typical Raman spectra from the heating of FeO, calcite and water near 5 GPa. The broad O-H stretching vibration of ice VII or liquid water near 3200 cm^{-1} is ubiquitous in these H_2O-rich samples. (a) Raman spectrum produced by heating FeO, calcite and water to 1500°C at 5.7 GPa. In isolated regions methane is the dominant Raman-active component. (b) A spectrum produced after resistively heating to 600°C and a decrease in pressure to ~2 GPa; the production of methane is clearly indicated by the C-H stretching vibration at 2932 cm^{-1}.

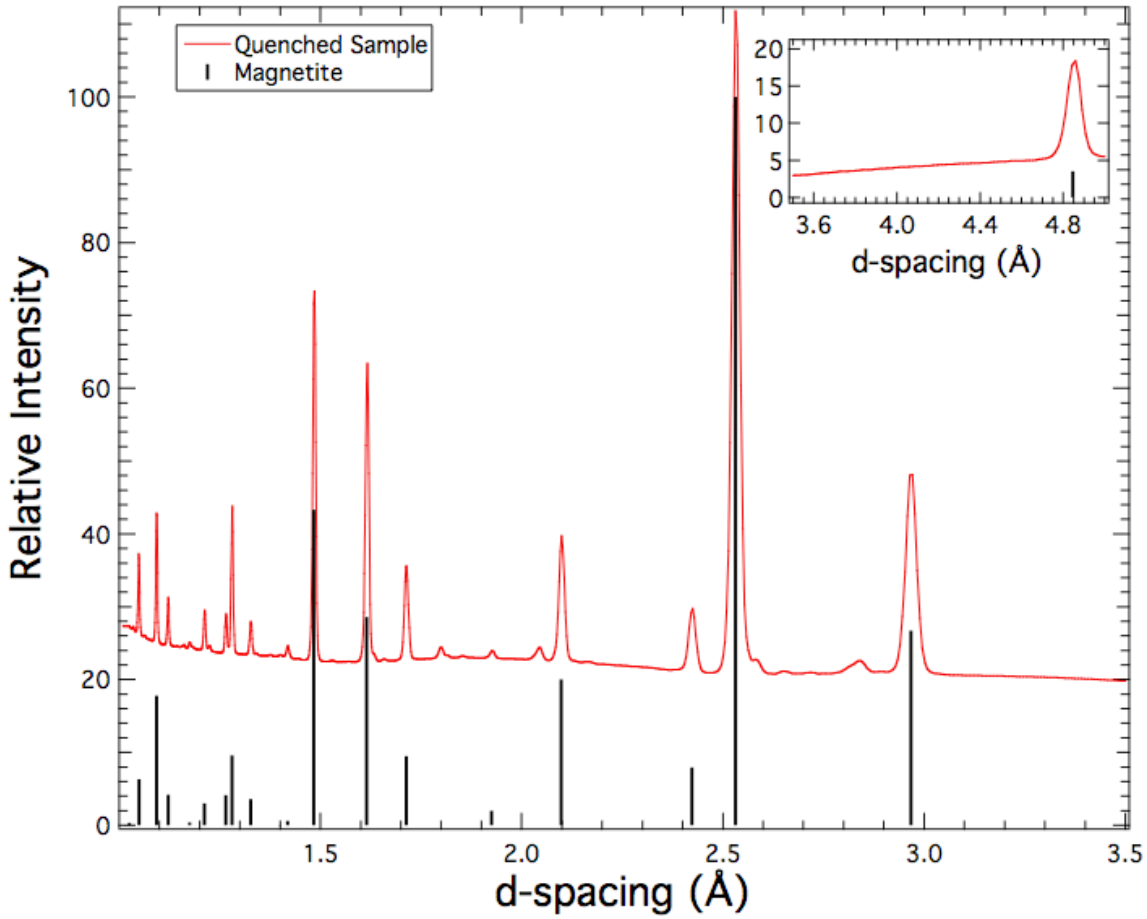

Figure 2: Temperature and pressure quenched X-ray diffraction pattern after external heating to 600° C at 5 GPa. Fe_3O_4-magnetite dominates the spectrum; weak lines suggest a Ca-Fe oxide.

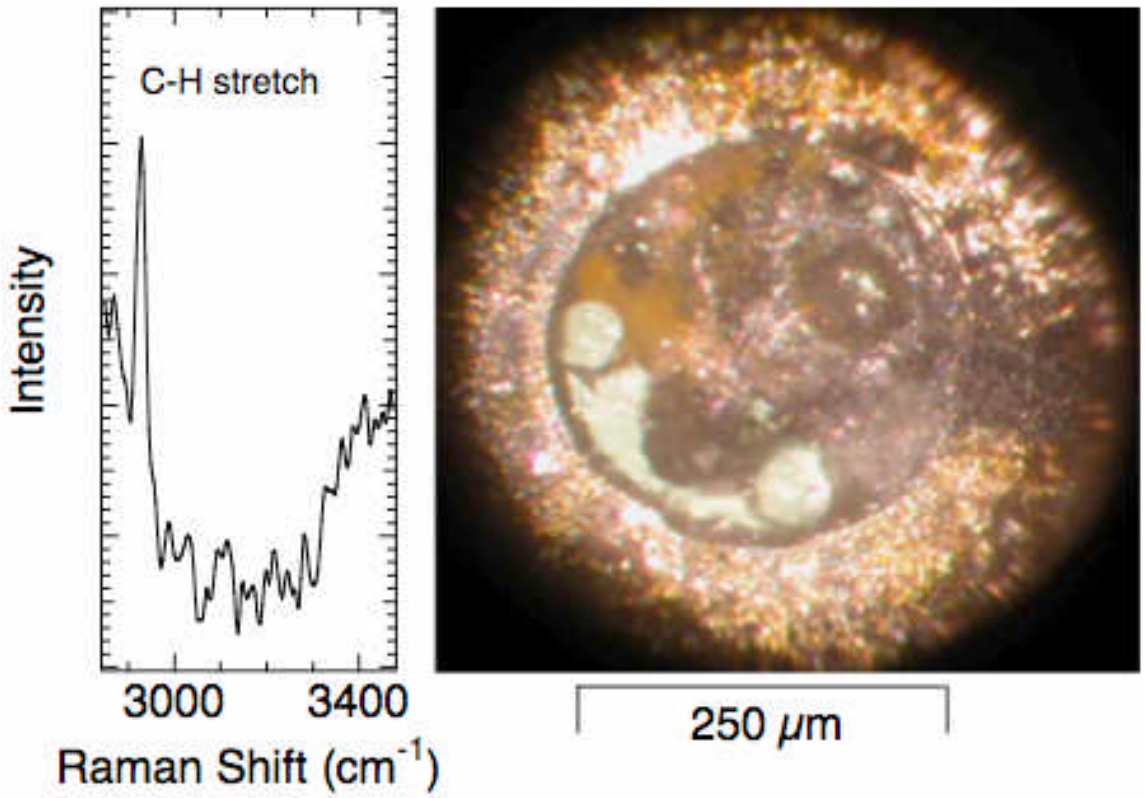

Figure 3: Raman spectra of low-pressure bubbles (shown on right) formed upon decompression to approximately 0.5 GPa after laser heating at 5.7 GPa. Note the absence of O-H stretching vibrations because the bubble has displaced the surrounding H_2O. Bubbles are visible near the bottom, left side, and slightly right of center.

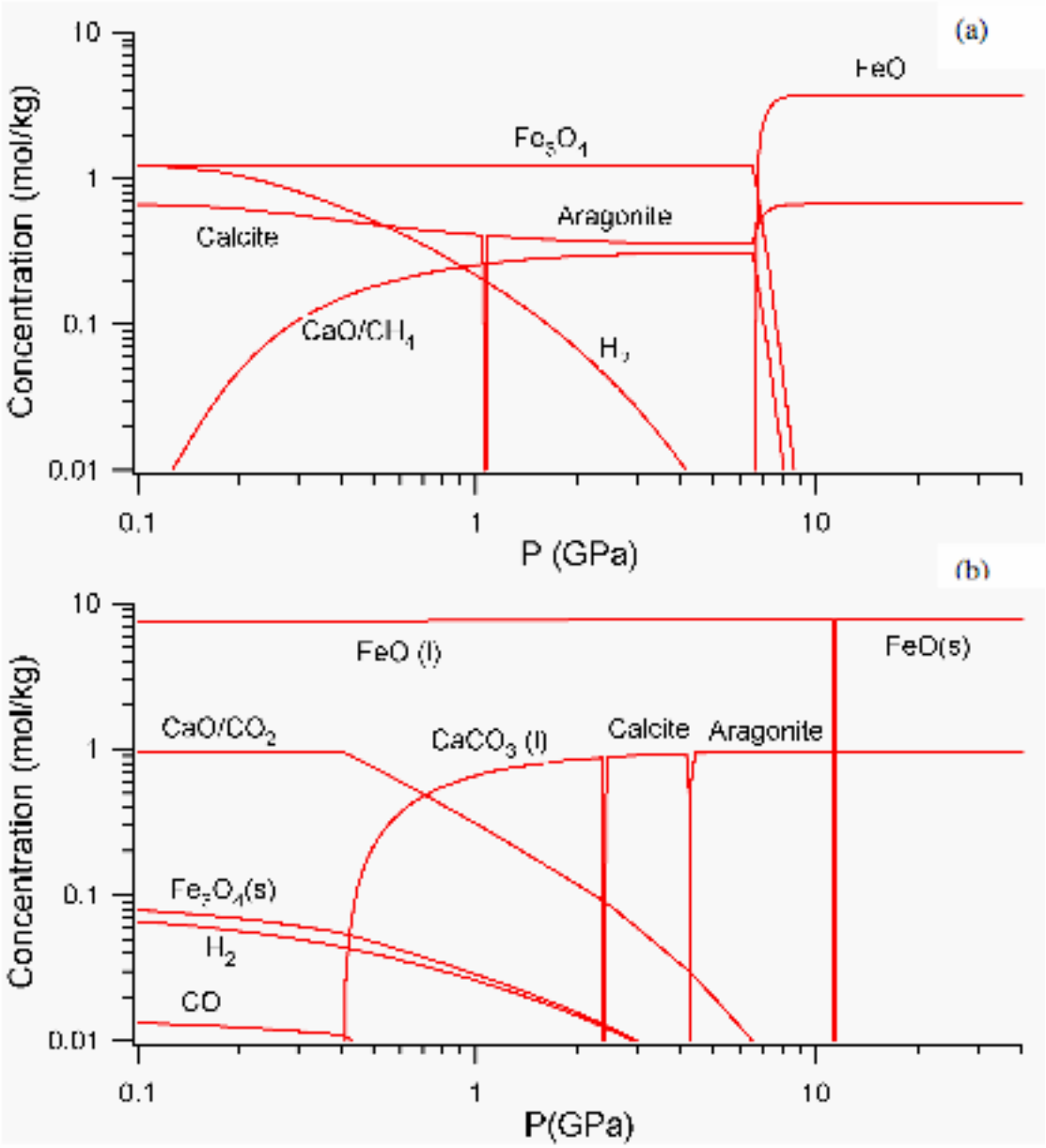

Figure 4: Results of thermochemical calculations. Concentrations at (a) 500º C and (b) 1500º C. CH_4 is predicted to be prevalent at temperatures below 1200º C, but H_2 is expected to become dominant at higher temperatures.